Jason-1 / Jason-2 metocean comparisons and monitoring

Graham D. Quartly
National Oceanography Centre, Southampton, Empress Dock
Southampton, Hants, SO14 3ZH, UK (gdq@noc.soton.ac.uk)

(This is the original version submitted to *Marine Geodesy* Jason-2 special issue 1st Dec 2009; for final version consult journal)

Abstract

The initial tandem phase of the Jason-2 mission is important for the calibration of the entire altimetric system, not just the records of sea surface height. However, as well as allowing a bulk comparison of metocean parameters such as wave height and backscatter strength (used to infer wind speed), it affords a more detailed opportunity to understand the artefacts within each instrument. The wave height comparison shows no bias between the instruments, with the mismatch error of consecutive points independent of one another. The backscatter difference is not a simple offset, but has a trend with weak non-linear variations. The technique for backscatter monitoring using K_u-/C-band differences is validated during the tandem phase, and extended to show 59-day oscillations in Jason-1 data, probably associated with spacecraft manoeuvres.

1. Introduction

Altimeter waveforms returns from a homogenous surface have a characteristic shape that is readily modelled in terms of a few parameters. Assuming the operating characteristics of the altimeter are well known, some key geophysical variables can be retrieved to a high accuracy (Brown 1977; Hayne 1980). The amplitude of the waveform is used to determine the normalised backscatter strength, σ^0, the slope of the leading edge is used to derive wave height, H_s, and the position of the leading edge gives the range, from which sea surface height (SSH) is derived. A further parameter estimated from fitting a simple model to the waveform is the slope of the trailing edge. Physically, this was expected to be related to the deviation of the altimeter boresight from nadir, and consequently changes in this slope are referred to in terms of ψ^2, the square of the mispointing angle; in practice surface inhomogeneities have a more pronounced effect leading to sharp variations between positive and negative values of this term.

Altimeters are used to study a wide range of metocean measurements — not just wave height and wind speed, but other derived parameters such as wave steepness and period (Mackay et al. 2008). Furthermore the different signal backscatter strengths at K_u-band and C-band have been used in rain detection algorithms (Quartly et al. 1996; Quartly 2004; Tournadre 2004) and in estimating air-sea gas transfer (Frew et al. 2007). In order to ensure that possible long-term trends associated with climate change can be detected, it is important to assess any difference in performance between the two altimeters, as well as monitoring for any gradual degradation once the cal/val period is over.

Analysis of the near-simultaneous records of TOPEX and Jason-1 during the Jason-1 cal/val phase in January-August 2002 helped clarify many of the differences between those two instruments, including the large offset in the values for σ^0 (2.40 dB at K_u-band, 0.72 dB at C-band) and some dependence upon ψ^2 (Quartly 2004). These comparisons were between two significantly different instruments: TOPEX emitting ~4500 K_u-band pulses per second using a travelling wave tube amplifier, with Jason-1 producing ~1800 pulses per second via a solid state amplifier. More importantly, these two used different waveform processing techniques to retrieve the geophysical parameters, with the TOPEX analysis at that time involving ratios of various gates (series of waveform bins), whilst Jason-1 had a modelled waveform fitted using MLE-3 (Maximum Likelihood Estimator with 3 degrees of freedom).

The comparison for the cal/val phase for Jason-2 (July 2008 to January 2009) should be much easier, as the altimeter hardware is almost identical, and data retrieval for both is via the same processing chain, involving a 4th order MLE because of the occasional large mispointing values noted early on in the Jason-1 mission (Amarouche et al. 2004). The most pertinent differences between the two Jason altimeters are that i) the raw waveform data telemetered from Jason-1 used some bin averaging in the trailing edge in order to reduce throughput, whereas all 104 waveform bins are transmitted for Jason-2, and ii) a number of different on-board trackers have been used for Jason-2 (although that should not necessarily impact upon the quality of retrievals from the ground-based reprocessing).

In the following section I describe the data sources used and the editing criteria applied, with brief comparisons of the waveform data from which other parameters are derived. Section 3 then displays the simple match-up of 1 Hz H_s and σ^0 data, with section 4 looking at the utilization of simultaneous dual-frequency data for σ^0 monitoring. Some initial conclusions are presented in section 5.

2. Data sources and quality control

Jason-2 was launched on 20th June 2008, with the earlierst available data coming from 4th July (part way through cycle 000). It was in an orbit 54.5 s behind Jason-1, with occasional manoeuvres of both satellites to maintain their ground tracks within 1 km of each other. This tandem formation was maintained until 26th January 2009, when Jason-1 was moved from that orbit into a different 'interleaved' one. There are simultaneous data from the two altimeters for most of the time that both were in the tandem phase, except for a 10-day period in August when Jason-1 was in a safehold mode.

The majority of the data used in this paper were from the RADS database (http://rads.tudelft.nl/rads/rads.shtml) enabling records to be retrieved with the most up-to-date corrections already applied. [In that database, gross adjustments to σ^0 have been applied to match Jason-1 values with those from TOPEX; those corrections have been removed here, so that values used match those on the original Jason-1 GDRs (Geophysical Data Records).] In previous analyses I have used the 20 Hz records and recomputed 1-second averages with the best spatial match between Jason-1 and Jason-2 (Quartly 2009a,b); this is not needed here because the real wave height varies on scales larger than that traversed in one second, and the backscatter data have had an empirical adjustment applied (Quartly 2009a) that minimises small-scale variations in σ^0. The adjustment is defined by:

$$\sigma^0_{adj} = \sigma^0 - \alpha\,(\psi^2 - \psi^2_{lo}) \qquad (1)$$

where the proportionality constant, α, is 11.30 for Jason-2 and 11.14 for Jason-1 (Quartly 2009b) and ψ^2_{lo} is a long-term average of ψ^2 (here defined via a 140-sec moving average). Quartly (2009b) also implemented an adjustment for Jason-1 for the long-term mispointing, as that satellite had periodic excursions to large values of ψ^2_{lo}. Here, where I am concentrating on a high accuracy intercomparison of the two satellites, and subsequent investigation of long-term changes, I have ruthlessly discarded any data with a large value for ψ^2_{lo}, keeping only data less than 0.015 deg^2 for Jason-1 and in the range 0.006 to 0.018 deg^2 for Jason-2, which has a different distribution (Fig. 2d of Quartly 2009b). Data are also discarded if poleward of 55°S/N (in order to minimise contamination by sea-ice within the footprint), or if in shallow water or if the microwave radiometer indicates nearby land or significant rain (liquid water path ≥ 0.2 kg m^{-2}).

To inform subsequent comparisons, a brief analysis was made of simultaneous waveform data from the Jason-1 and Jason-2 altimeters. The analysis shown here is from Jason-2 cycles 008-010 (Jason-1 cycles 247-249), when the on-board tracking is controlled by the median tracker (rather than the DIODE/DEM coupled mode that initially produced lots of movement of the waveform within the window). To compare the waveforms accurately, a large number of waveform ensembles were averaged. [This crude approach may not be valid for the leading edge, where movement of the waveform will smear out the sharpness of features.] Data were considered in 10 s ensembles for which both the H_s and σ^0 varied little, and for which a full 200 waveforms were present for both Jason-1 and Jason-2. Then those ensembles for given wave conditions were averaged together.

Figure 1 shows the mean waveform shape observed by the two altimeters for conditions when H_s=2m. Their shapes are very similar, even down to the slight undulations along the trailing edge. The inset, focussing on the leading edge, shows that the mean waveform for Jason-2 is ~0.1 bins to the right of that for Jason-1. As the two curves in Fig. 1a have been scaled to have a waveform bin total of unity, the slight lag for Jason-2 leads to its depicted strength on the trailing edge being minutely greater. However, this difference is not uniform across the waveform. The percentage difference between the two is shown by the solid line in the lower plot. An almost identical trace is found when considering ensembles averaged at any conditions between H_s=1m and H_s=6m (which would represent very different oceanographic regions).

The consistent sharp features in the second half of the trailing edge probably relate to an artefact of the averaging and subsequent expansion of Jason-1 bins in groups of five. The broad trend in Fig. 1b, again consistent across all wave heights, indicates small differences in the shape of the trailing edge, Jason-2 having a flatter slope than Jason-1 over the first half, and a steeper slope in the second half. The square of the mispointing angle, ψ^2, is derived from the slope within the trailing edge. The observed subtle difference in waveform characteristics may explain why the mean mispointing angle for Jason-2 is 0.0112 deg^2, whereas Jason-1 has a modal value nearer zero, although for particular cycles the mean may be considerably greater (see Fig. 2e of Quartly 2009b) due to genuine attitude problems with the spacecraft. Finally, the expansion of the Jason-1 waveform bins give a perfectly linear continuation at the end of the waveform, whereas the actual measurements for Jason-2 show a consistent drop off of 1-1.5% for the final bin, which may be a remnant effect induced by the circular Fourier Transform in the processing (see ERS-1 examples in Quartly et al. 2001).

In the succeeding sections I look at the agreement in the derived geophysical parameters from Jason-1 and Jason-2.

3. Comparisons of wave height and backscatter strength

For these comparisons, Jason-1 was used as the reference dataset, and statistics binned according to the values from this instrument. Figure 2 shows the comparison of wave height data, considered in 0.5 m intervals. The top plot is a 2-D histogram (with logarithmic scaling), indicating that the most populous interval is for H_s=2±0.25 m, and that the differences for Jason-2 relative to Jason-1 are symmetrically spread, with a mean deviation very close to zero and the vast majority of measurements agreeing within 0.4m (dashed lines showing ±2 standard deviations). Note that these data have been selected to be free from effects of ice, land or rain, so no extreme outliers should be expected. The middle plot shows the result upon applying a 9-sec moving average to the data. The r.m.s. deviation between the two altimeters' records decreases by almost exactly a factor of three, consistent with the errors between successive records being independent i.e. there are no slowly-varying factors leading to a slight bias between the two. Indeed, the difference between the 1 Hz data from the instruments is smaller than the typical along-track variation between records 5.6 km apart (Fig. 2c).

A similar two-dimensional histogram is shown for the σ^0_{Ku} backscatter values in Fig. 3a. The relative assessment of the instruments is more complicated than for wave height. Not only is there a mean offset of -0.28 dB, but the offset varies by 0.06 dB from low to high σ^0 values. The r.m.s. deviation about this mean is 0.05 dB, with such a small value being due to the correction for high frequency variations in ψ^2 (Fig. 3 of Quartly 2009b). Figure 3b in this paper concentrates on the mean relationship, and notes that there is a slight variation with wave height: ~0.007 dB per 1 m change in H_s. There is a greater slope to the fitted line at C-band (Fig. 3c), but the variations with wave height are less coherent. [Note that the Jason-2 GDRs also contain an alternative definition of σ^0 based on a sea-ice model; the offset between the ocean and ice definitions of σ^0 vary slightly with wave height (Quartly 2009c).] Quartly 2009c) noted that the standard deviation of the σ^0 mismatch between instruments (after bulk rescaling) is less than the r.m.s. difference between neighbouring observations; such good agreement between instruments 55 s apart was found even when rain was likely to be present.

4. Long-term σ^0 monitoring

The highly correlated σ^0 observations at K_u- and C-band are key to techniques to develop rain-flagging and rain-rate quantification from altimeter data (Quartly et al. 1996, Quartly et al. 1999; Tournadre 2006). Figure 4 shows the envelope of simultaneous dual-frequency observations for Jason-1 (indicated by mean and dashed lines for ±2 standard deviations). Curves shown here have been calculated using points for which Hs is between 1.5 and 2.5 m, because wave height has an effect upon the mean relationship (Elfouhaily et al 1998), although for Jason-2 data thee is minimal offset near near the peak of the curve (see Fig. 3e of Quartly 2009c). For all the work in this section, the Jason-2 σ^0 values have been rescaled according to the offsets and slopes illustrated in Figs 3b & c. Thus, not surprisingly, the mean σ^0_{Ku}- σ^0_C relationship for Jason-2 is close to that for Jason-1, but with some difference in shape due to the non-linear relationships shown earlier. The inset shows the region where the slope is near zero (i.e. the mean value of σ^0_{Ku} changes at the same rate as σ^0_C). Fortuitously, this coincides with a large density of observations, so that any change in the mean offset between the two frequencies can be reliably determined just using observations in the shaded region. Here I focus on the conditions for which σ^0_C is between 15.3 and 15.6 dB for both Jason-1 and rescaled Jason-2 data. [Similar results, albeit with an offset are noted if the second shaded region is used for rescaled Jason-2 values.]

In many cases, a single pass of data is enough to constrain this difference quite accurately, and thus follow short-term changes in instrument performance (Quartly 2000). In what follows, I examine four different σ^0 records (Jason-1 and Jason-2 observations at K_u- and C-band), using statistics averaged over individual days.

The top plot of Figure 5 shows the daily variations in the offset of Jason-2 relative to Jason-1 (once gross offset and trend have been applied). By definition, both series have an average of zero, but they do show periods when the mean offset is of order 0.03 dB for weeks at a time, especially for C-band. It is not immediately clear whether the error is in data from the new altimeter or the reference one. Figure 5b shows the varying height of the peak illustrated in Fig. 4. Apart from a slight downward trend in July, the mean bias for Jason-2 stays between -1.55 and -1.50 dB. Conversely, a pronounced change of nearly 0.1 dB occurs for Jason-1 in September, indicating that the C-band offset noted for Jason-2 in this month (top plot) is due to changes in the values recorded by Jason-1. Another period of increased K_u-/C-band differences for Jason-1 is noted in November.

Figure 4c shows two ways of constructing the 4-way comparison, $\Delta\sigma^0_{(4)}$, defined by:

$$\Delta\sigma^0_{(4)} = \sigma^0_{Ku\_J2} - \sigma^0_{Ku\_J1} - \sigma^0_{C\_J2} + \sigma^0_{C\_J1} \qquad (2)$$

where 'J1' and 'J2' in the suffices indicate whether Jason-1 or Jason-2 data. There is an offset of ~0.04 dB between the two curves, because although Jason-2 data have been linearly rescaled to match Jason-1 data, the peaks in the left-hand shaded region of Fig. 4 differ by 0.04 dB. Clearly if exactly the same narrow set of observations are used in all four comparisons shown in Figs. 5a & b, then the two 4-way comparisons will coincide. What is significant is that the comparisons using the K_u-/C-band relationship not only use far fewer data points, but do not need to have coincident observations by the two altimeters. For example, performing the comparison using dual-frequency Jason-1 data from the northern hemisphere and Jason-2 data from the south only makes a mild reduction in the quality of the comparison. This is because the position of the apex of this curve is a more stable estimator of an altimeter's σ^0 performance than is the mean value over the same period (as that can vary according to changes in global average wind conditions).

Consequently the position of this peak can be used to intercompare Jason-1 and Jason-2 observations when they are not observing the same parts of the ocean, as is the case during the interleaved mission. This study also allows a re-evaluation of the Jason-1 altimeter for the duration of its mission. Daily averages of the K_u-/C-band offset have been calculated for every day available for both the Jason-1 and Jason-2 missions, with a 19-day smoother applied to reveal the longer period changes. Figure 5b had shown a change in Jason-2 during July 2008; this feature is more apparent after the smoothing (Fig. 6). The Jason-1 data show a gradual change of about 0.04 dB over 8 years (although this is not clear if it is in σ^0_{Ku}, σ^0_C or a combination of both). What is more striking is the almost periodic oscillations for Jason-1, with a peak to peak variation of 0.06 dB. The added dotted lines on the figure are every 59 days, and match with most, although not all, of the peaks; this includes the features in September and November 2008 (Fig. 5b), which suggests that the perceived effect is mainly at C-band.

This seems likely to be due to spacecraft manoeuvres, with the Jason-1 craft being rotated from yaw-steering mode to fixed yaw mode approximately every 60 days. This is done to control the solar illumination on the spacecraft, hence the period coinciding with a known alias of the solar day. Through a comparison of Jason-1 altimetry and wind vectors from weather reanalyses, Tran and Chapron (2006) had shown that the direction of wind would have a small impact (~0.05 dB) at wind speeds of around 6-7 ms^{-1} (which correspond to the $\sigma^0{}_C$ values around 15.3-15.6 dB used here). The results in Fig. 6 seem to confirm their finding.

5. Summary and conclusions

Comparisons of mean waveforms from the Jason-1 and Jason-2 altimeters reveal them to have very much the same shape, including the slight ripples on the trailing edge (Fig. 1a). Examining the percentage difference between the two (Fig. 1b) shows some minor artefacts of the Jason-1 waveform descoping, plus a weak bend along the trailing edge. This latter effect may explain why the long-term mispointing angles for Jason-2 are greater than 0.01 deg^2, without the spacecraft necessarily having an attitude problem. The shape of the leading edge for the two instruments appears identical, and is reflected in the fact that the H_s estimates from Jason-2 are unbiased with respect to Jason-1 (Fig. 2a). The r.m.s. difference between the two instruments' estimates is 0.15 m at low wave heights, rising to 0.25 m at H_s=7m. These values appear to be fractionally larger than the std. dev. of mismatch between TOPEX and Jason-1 values during their overlap period, but there were notable biases between those two instruments, with some features coinciding with the location of TOPEX gate boundaries (Fig. 4 of Quartly 2004).

The intercomparison of Jason-1 and Jason-2 σ^0 values is surprisingly complicated, given the strong similarities in hardware and processing. Not only does the best-fit line through simultaneous σ^0 data show a slight trend (1.9% for $\sigma^0{}_{Ku}$, 2.9% for $\sigma^0{}_C$), but there are also domains where the mean relationship departs from this straight line by up to 0.05 dB. This is still a small offset (amounting typically to a wind speed error of 0.1-0.2 ms^{-1}), but is worth noting in the context of looking for gradual changes in the global climate.

Comparisons between instruments are useful in permitting one instrument to be calibrated to the records of another, but cannot address the issue of long-term secular changes in instrument performance. Quartly (2000) introduced the idea of monitoring σ^0 performance of an altimeter through its dual-frequency characteristics, finding the necessary adjustments in $\sigma^0{}_{Ku}$ and $\sigma^0{}_{Cu}$ to maintain calibration. Here, evaluation has only been of the simplified idea of monitoring the difference in K_u- and C-band values. There was a change in Jason-2 of 0.05 dB during the first month of operation, which comparisons with Jason-1 suggest was in the K_u-band (Fig. 5a). Jason-1 has shown a very gradual drift in the apex of $\sigma^0{}_{Ku}$-$\sigma^0{}_C$, which is slower than that noted for A-side of TOPEX (Fig. 3a of Quartly 2000), but the most startling observation is of 0.06 dB oscillations in their difference, with an almost regular period of 59 days. This is tentatively linked with changes in the spacecraft orientation as it seeks to maintain thermal stability in space.

Acknowledgements

The waveform data were obtained from CLS FTP server under the OSTST-approved project, 'TRIDENTt II'; RADS provided the 1 Hz data.

References

Amarouche, L., P. Thibaut, O.-Z. Zanife, J.P. Dumont, P. Vincent, and N. Steunou, 2004. Improving the Jason-1 ground tracking to better account for attitude effects. *Mar. Geod.* 27: 171-197.

Brown, G.S., 1977. The average impulse response of a rough surface and its applications. *IEEE J. Ocean. Eng.* 2 (1): 67–74.

Elfouhaily, T., D. Vandemark, J. Gourrion, and B. Chapron, 1998. Estimation of wind stress using dual-frequency TOPEX data. *J. Geophys. Res.* 103: 25 101-25 108.

Frew, N.M., D.M. Glover, E.J. Bock, and S.J. McCue, 2007. A new approach to estimation of global air-sea gas transfer velocity fields using dual frequency altimeter backscatter. *J. Geophys. Res.* 112: C11 003.

Hayne, G.S., 1980. Radar altimeter mean return waveforms from near-normal incidence ocean surface scattering. *IEEE Trans. Antennas Propag.* 28 (5): 687–692.

Mackay, E.B.L., C.H. Retzler, P.G. Challenor, and C.P. Gommenginger, 2008. A parametric model for ocean wave period from Ku band altimeter data. *J. Geophys. Res.* 113: C03 029, doi: 10.1029/2007JC004438.

Quartly G.D., 2000. Monitoring and cross-calibration of altimeter σ^0 through dual-frequency backscatter measurements. *J. Atmos. Oceanic Tech.* 17: 1252-1258.

Quartly, G.D., 2004. Sea state and rain: A second take on dual-frequency altimetry. *Mar. Geod.* 27 (1-2): 133-152. & 27 (3-4): 789-795.

Quartly, G.D., 2009a. Optimizing σ^0 information from the Jason-2 altimeter. *IEEE Geosci. Remote Sens. Lett.* 6 (3): 398–402.

Quartly, G.D., 2009b. Improving the intercalibration of σ^0 values for the Jason-1 and Jason-2 altimeters. *IEEE Geosci. Remote Sens. Lett.* 6 (3): 538–542.

Quartly, G.D., 2009c. Improving the altimetric rain record from Jason-1 & Jason-2, *J. Geophys. Res.* (in press) available at http://eprints.soton.ac.uk/69130

Quartly, G.D., T.H. Guymer, and M.A. Srokosz, 1996. The effects of rain on TOPEX radar altimeter data. *J. Atmos. Ocean. Tech.* 13 (6): 1209–1229.

Quartly, G.D., M.A. Srokosz, and T.H. Guymer, 1999. Global precipitation statistics from dual-frequency TOPEX altimetry. *J. Geophys. Res.* 104 (D24): 31 489–31 516.

Quartly, G.D., M.A. Srokosz and A.C. McMillan, 2001. Analyzing altimeter artefacts: statistical properties of ocean waveforms. *J. Atmos. Oceanic Tech.* 18: 2074-2091.

Tournadre, J., 2004. Validation of Jason and Envisat altimeter dual-frequency rain flags. *Mar. Geod.* 27: 153-169.

Tournadre, J., 2006. Improved level-3 oceanic rainfall retrieval from dual-frequency spaceborne radar altimeter systems. *J. Atmos. Oceanic Tech*. 23: 1131-1149.

Tran N, and B. Chapron, 2006. Combined wind vector and sea state impact on ocean nadir-viewing Ku- and C-band radar cross-sections. *Sensors* 6 (3): 193-207.

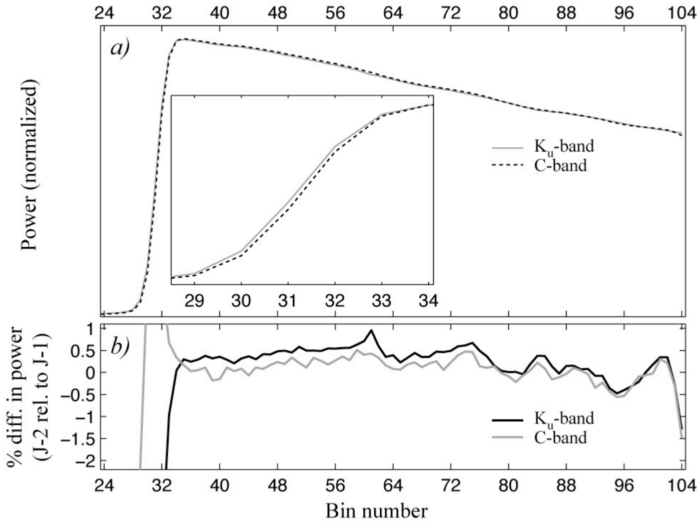

FIGURE 1. Comparison of mean waveform shapes for Jason-1 and Jason-2 altimeters. a) K_u-band waveform at H_s=2m (calculated from 458 10-second averages, for which mean H_s = [1.75m,2.25m]. Inset shows zoom on leading edge. b) Percentage difference in power of Jason-2 relative to Jason-1 for both K_u- and C-band at H_s=2m.

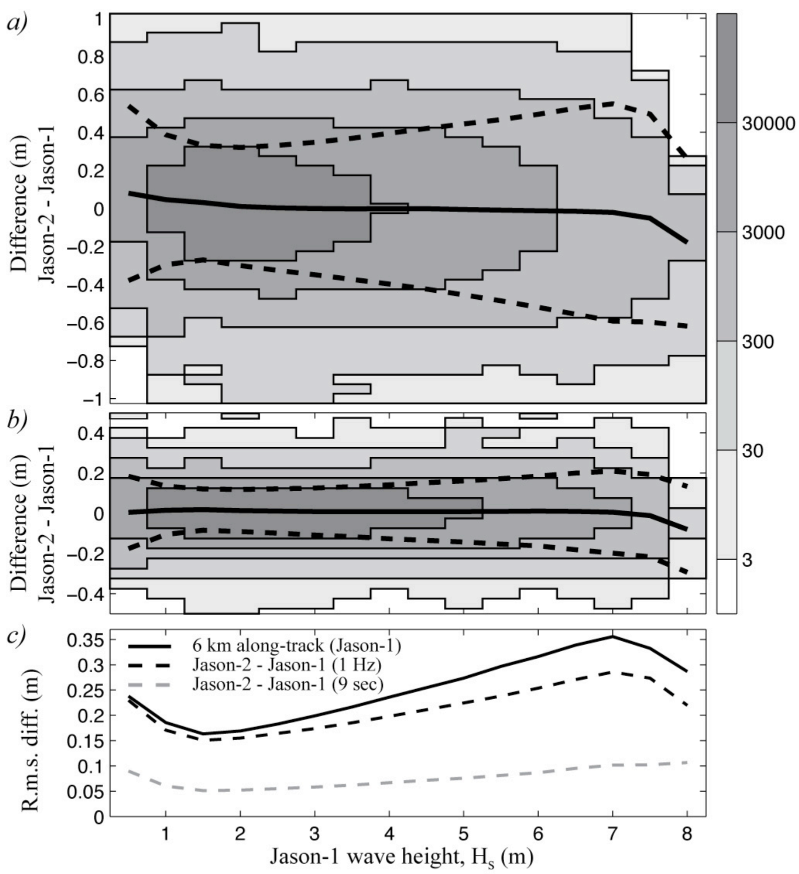

FIGURE 2. Two-dimensional histogram of H_s differences between Jason-1 and Jason-2 1 Hz records. Added lines show mean and ±2 std. dev. b) As above but for 9-second running average. c) R.m.s. difference in wave height for records 6 km apart along-track (solid line) and for collocated comparisons of the two altimeters (dashed lines).

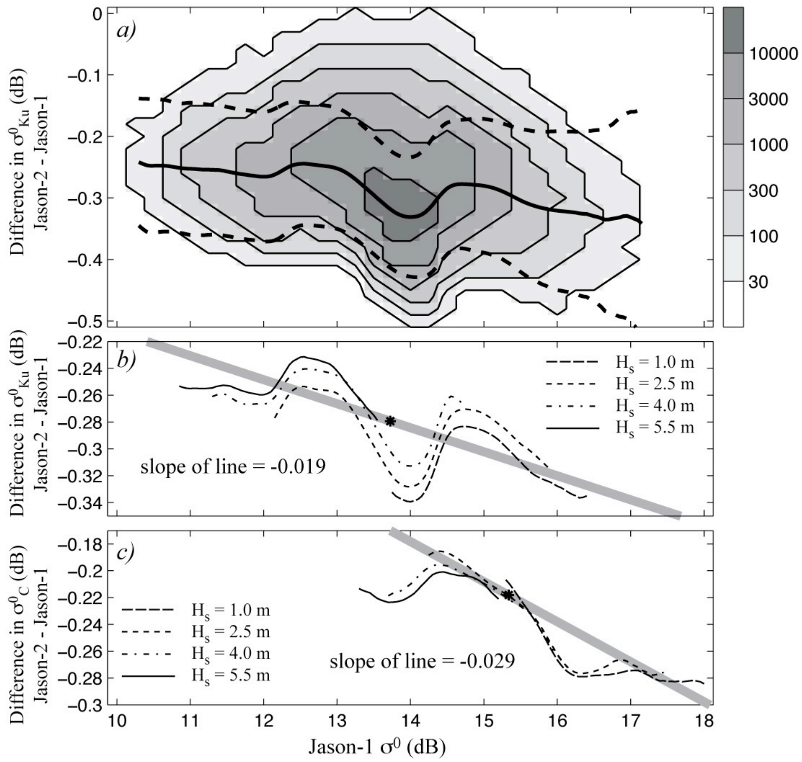

FIGURE 3. a) Two-dimensional histogram of σ^0_{Ku} differences between Jason-1 and Jason-2 1 Hz records. Added lines show mean and ±2 std. dev. b) Mean difference between σ^0_{Ku} values as a function of wave height. Thick line shows fitted trend, with asterisk indicating the mean. c) Same for C-band.

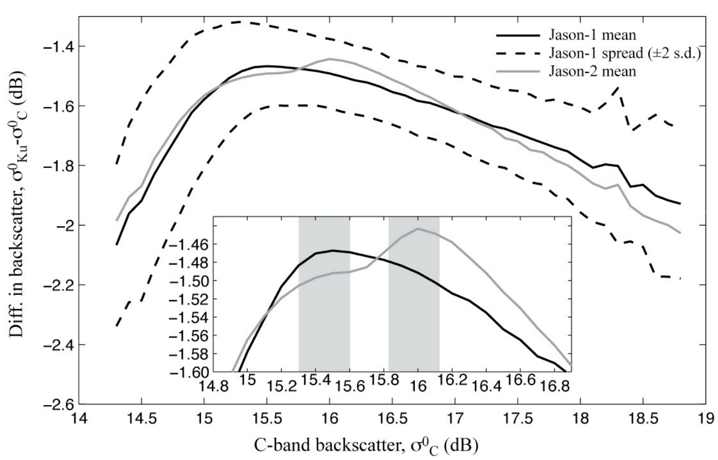

FIGURE 4. Comparison of simultaneous K_u- and C-band σ^0 values, with solid line showing mean relationship and dashed lines indicating ±2 std. dev. The inset focuses on the region where the relationship is nearly flat.

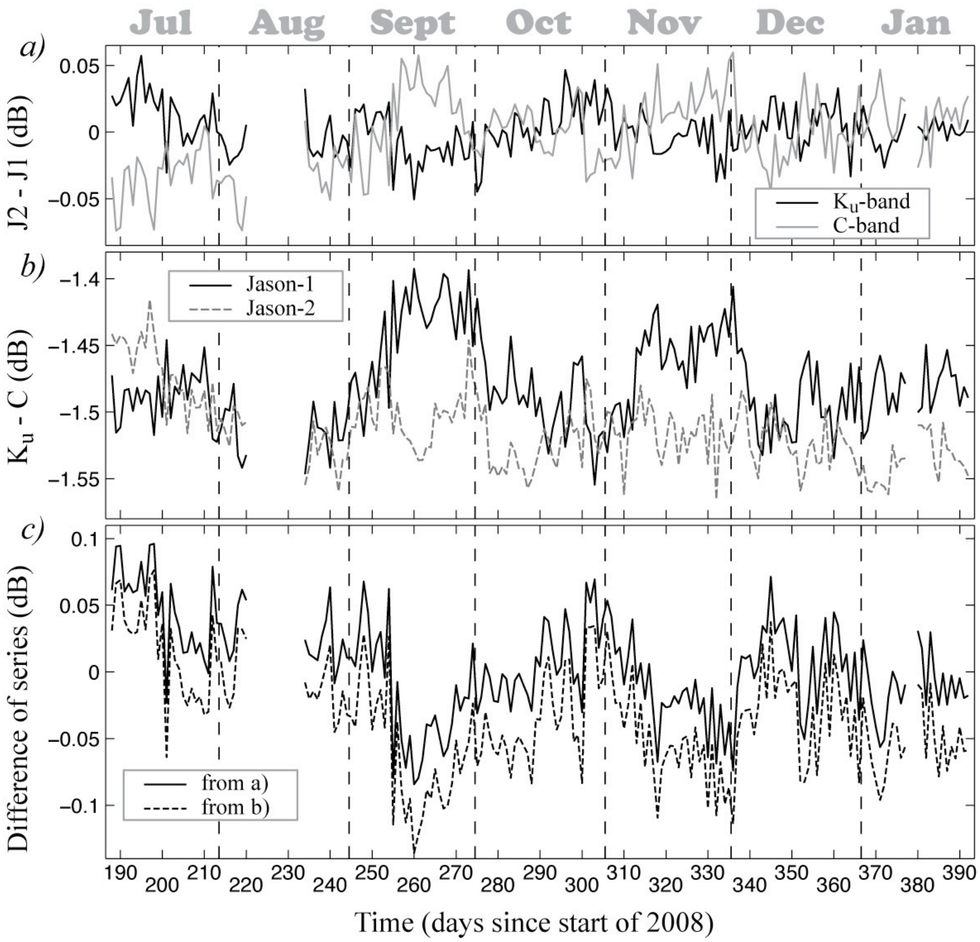

FIGURE 5. Daily averages of σ^0 statistics for the Jaason-1/2 tandem mission. a) Mean offset of collocated observations, b) Difference in frequency band measurements for σ^0_C=[15.3, 15.6] dB (left-hand shaded region identified in Fig. 4). c) $\Delta\sigma^0_{(4)}$ evaluated as the difference of series shown within previous sub-figures.

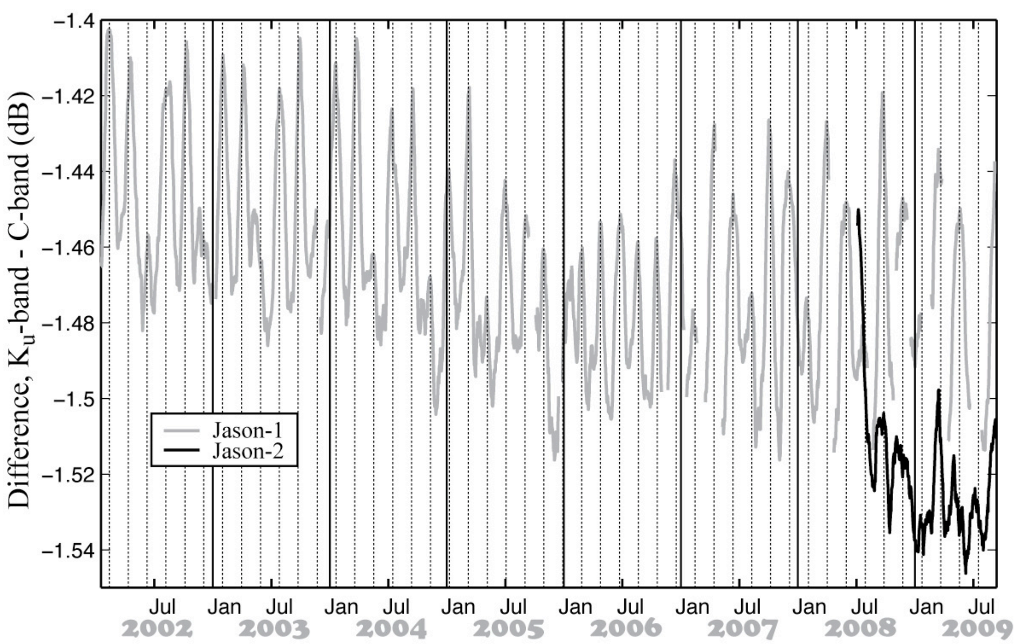

FIGURE 6. Difference in frequency band measurements for σ^0_C=[15.3, 15.6] dB after 19-day smoother applied. (The dashed lines are every 59 days.)